Natural Frequency Analysis of a ABS Material Drone Ground Moving System

IULIAN NICOLA*, DANIEL TURCANU, TUDOR PRISECARU, CRISTIAN PREDOI, MIHAELA CRISTINA CIOBANU
University Politehnica of Bucharest, Romania, 313 Splaiul Independentei,060042, Bucharest, Romania

The paper presents comparative analysis for different solutions for the body of an internal spur gear used in a ground movement system of a drone with aerial and terrestrial movement capability. The comparative analysis is made from natural frequencies perspective and the purpose of the analysis is to reduce the weight of the drone without affecting its mechanical resistance and vibrational characteristics.

Keywords: internal spur gear, modal analysis, natural frequencies, drone

The purpose of this paper is to present the results of researches conducted in order to identify solutions for reducing the weight of a drone and, at the same time, to maintain its mechanical resistance and vibrational characteristics.

The drone was designed to be able to move both on the air and on the ground and to be equipped with multispectral sensors.

There are many projects regarding only terrestrial drones or aerial drones, but this drone combines the advantages of the both systems (aerial and terrestrial movement): high mobility - it can reach the area of interest by alternation of the two movement types (aerial and terrestrial); the observation of interest points can be accomplished from close proximity due to the reduction of noise level in case of ground movement compared with the aerial movement; it increases the effective time used for observation. The ground movement consumes less energy than aerial movement.

The ground moving system of the drone consists from an internal spur gear, which is in contact with the ground and which geared, in the upper side, with a spur gear mounted on the axis of an electrical motor. The weight of the drone is sustained with the help of two gears, identical with the one mounted on the motor axis, and support elements for the gears and motor. The internal spur gear transfers the power to the ground.

The three identical spur gears are positioned on the internal spur gear at 120° angles relative to each other.

The main characteristic of the ground moving system of the drone is that the wheel which is in contact with the ground is eccentrically motorized. The ground moving system of the drone is presented in the figure bellow.

The advantages of the design ground moving system are: it reduces to 70% the traction force necessary to cross obstacle and climb the slope; it doesn't need to use a reduction gear box. Because of the rotation speed and power of the electric motors for drones, the usage of a normal wheel impose the use of a reduction gear box; it reduces the weight of the assembly.

Theoretical consideration

The natural frequency of a structure only depends with the weight and the stiffness of the structure. If the stiffness of the structure increases, the natural frequency will increase. The same rule applies for the weight.

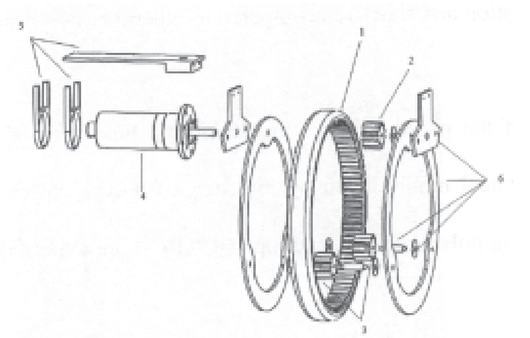

Fig. 1. Components of the ground moving system (1 – internal spur gear, 2 – spur gear mounted on the motor axis, 3 - spur gears for supporting the drone weight, 4 – brushless electrical motor, 5, support elements for the motor, 6 – fixtures elements)

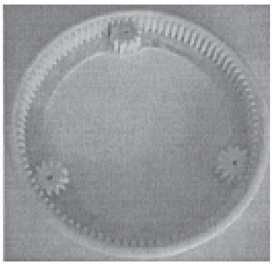

Fig. 2. Internal spur gear and regular spur gears made from ABS

During their researches, Wei Li, Yueming Li [1] found out that the natural frequencies decrease with an increase in temperature, while the mode shapes remain the same. Also, the thermal stress will reduce the stiffness of the structure, and the softening effect will reduce the natural frequency. In their paper it is found that the natural frequencies decrease with the uniform temperature rise, and the resonant amplitudes of vibration response and the sound pressure level response are reduced with the increase in temperature.

A.D. Lin, J. H. Kuang [2] studied the influence of gear parameters on the pinion life. They concluded that when in the case of pinion with fewer tooth number, negative profile-shifted factor and lower tooth hardness, the surface failure mode dominated. On the contrary, the break failure happened at high values of tooth number and tooth hardness, and positive profile shifted factor.

According to ISO/DIS 6336, the resonant frequency of a gear , and can be written as A.D. Lin, J. H. Kuang [2]:

---

* *email: iuliannicola@yahoo.com*

$$f_{so} = \frac{10^3}{2\pi N_1}\sqrt{\frac{K_s}{M_r}} \qquad (1)$$

where:

K_s is the mesh stiffness per unit tooth thickness;

M_r - the reduced mass per unit tooth thickness;

N_1 - the tooth number of gear 1.

$$M_r = \frac{M_1 M_2}{F(M_1 + M_2)} \qquad (2)$$

where:

M_1, M_2 is the effective masses of gear 1 and 2;

F - the tooth thickness;

The stiffness of a body is a measure of the resistance offered by an elastic body to deformation. Stiffness is a property of a structure. For an elastic body with a single degree of freedom the stiffness is defined as:

$$K = \frac{F}{\partial} \qquad (3)$$

where:

F is the force applied on the body;

δ - the displacement produced by the force along the same degree of freedom.

Timo Kiekbusch, Daniel Sappok [3] defined the combined torsional mesh stiffness K_m as the ratio of the input load *T* [Nm] and the driving gear hub rotation under load *T.E.* [rad] [4, 5]:

$$K_m = \frac{T}{TE} \qquad (4)$$

This definition can be used for the dynamic simulation of spur gear systems as it directly describes the relation between load torque and relative motion of the gears.

The torsional stiffness of a single gear can be defined using the assumption that the stiffness of body, teeth and contact zone can be considered to act like three springs in a row, resulting the fallowing equation for the combined stiffness *K* [3]:

$$K = \left(K_B^{-1} + K_T^{-1} + K_C^{-1}\right) \qquad (5)$$

where:

K_B^{-1} is the gear body stiffness,;

K_T^{-1} the tooth stiffness;

K_C^{-1} the contact stiffness.

The stiffness of the gear body is assumed to only depend on the following parameters: shaft radius r_s, dedendum radius r_d, face width *w* and Young's modulus *E*.

Different combinations of parameters were used to come to the following equation [3]:

$$K_B = c_B \cdot E \cdot w \cdot \ln(r_d - r_s)^{1,6} \cdot r_s^{1,6} \qquad (6)$$

Table 1

INTERNAL SPUR GEARS CHARACTERISTICS

	Weight	Volume	Density of the component	Moments of inertia: ($g \cdot mm^2$) taken at the center of mass form CAD model
Solid body internal spur gear	158.3 g	155196.326 mm^3	1020 kg/m^3	L_{xx} = 1646208.301 L_{yy} = 829507.894 L_{zz} = 829507.894
Solid body with holes internal spur gear	148 g		953 kg/m^3	L_{xx} = 1536866.689 L_{yy} = 774348.460 L_{zz} = 774348.775
Goffer type structure internal spur gear	137.454 g		885 kg/m^3	L_{xx} = 1431439.189 L_{yy} = 721540.971 L_{zz} = 721540.971

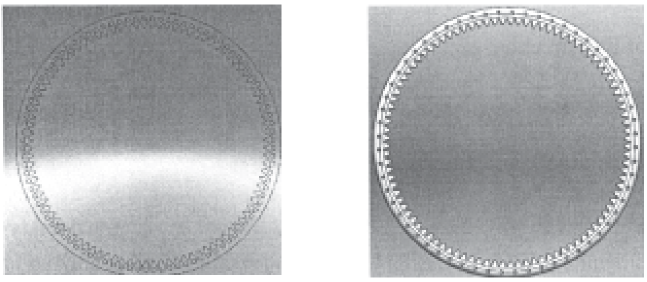

Fig. 3. Internal spur gear with a goffer type structure of the body (left) and internal spur gear with transversal holes (right)

Solution for reducing the weight of the ground moving system

Taking into consideration that the drone most me able to move both on the ground ant into the air, its weight is very important. From all the components of the ground moving system, the component with the highest weight is the internal spur gear.

In order to reduce the weight of the internal spur gear, two solutions were identified:

a) internal spur gear with a goffer type structure of the body (fig. 3). The goffer type structure is designed in the transversal plane and is realized by continuing the tooth's walls.

b) internal spur gear with transversal holes. In order to reduce the weight of the internal spur gear, there were made 60 transversal holes in a solid body internal spur gear, equally spaced. Bellow is a schematic representation of the solution.

Experimental determination of natural frequencies

In order to determine the natural frequencies of the two solutions presented above and for a solid internal spur gear, the gears were printed on a 3D printer using ABS material [6].

In the table 1 is presented the characteristics of the three solutions for the internal spur gear (solid body, goffer type holes and solid body with holes).

The natural frequency on radial and transversal direction were determined using TIRA VIB THS 50-180 vibration stand.

Radial natural frequency

In order to determine the radial natural frequency the fixture shown in figure 4 was used. The input acceleration given by the vibration stand was 3g. The response of the internal spur gear was measured radially in the opposite point of the internal spur gear (fig.4). The frequency varied continually from 10 Hz to 150 Hz.

The results are shown in table 2 and in figure 5.

Transversal natural frequency

In order to determine the transversal natural frequency the fixture shown in figure 5 was used. The input

Fig. 4. Determination of radial natural frequency

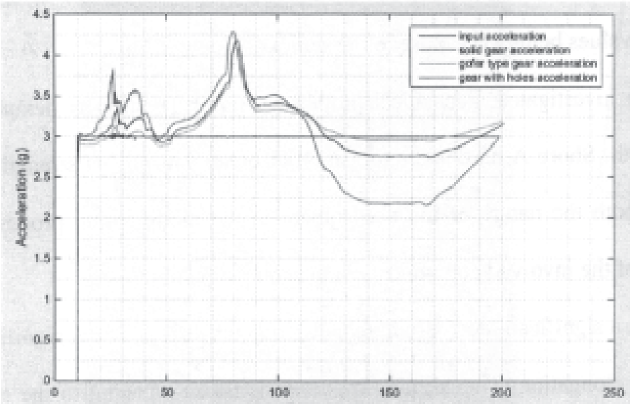

Fig. 5. The graphical representation of the radial response of the three internal spur gears

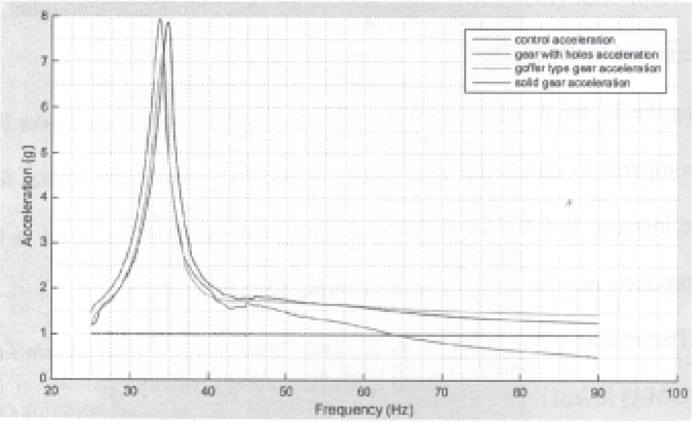

Fig. 6. The graphical representation of the transversal response of the three internal spur gears

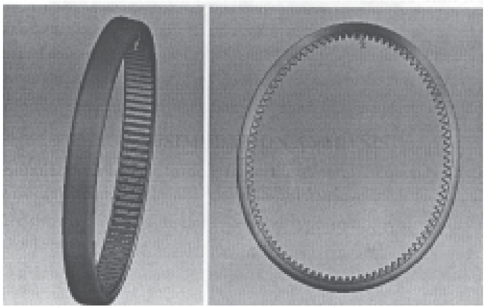

Fig. 7. The transversal and radial natural frequencies graphical representation from the results obtained during the simulation analysis

Table 2

RESULTS OF NATURAL FREQUENCIES OBTAINED DURING SIMULATION AND EXPERIMENTAL MEASUREMENT

	Direction	Simulation analysis	Measured
Solid body internal spur gear	Transversal	33.636 Hz	34.69 Hz
	Radial	84.94 Hz	79.96 Hz
Solid body with holes internal spur gear	Transversal	32.9 Hz	33.68 Hz
	Radial	86.502 Hz	81.68 Hz
Goffer type structure internal spur gear	Transversal	33.494 Hz	33.98 Hz
	Radial	84.825 Hz	81.18 Hz

acceleration given by the vibration stand was 1g. The response of the internal spur gear was measured along the vibration axis (transversal) in the opposite point of the internal spur gear (fig. 4). The frequency varied continually from 10 Hz to 150 Hz.

The results are shown in table 2 and in figure 6.

Simulation analysis

The simulation analysis to determine the natural frequency of the internal spur gear was done using modal analysis in SolidWorks.

The mesh used for this model is a solid type mesh, with a curvature based mesher and 4 Jacobian points.

The values for the natural frequencies obtained in the simulations are presented in table 2.

Although simulation analysis is useful and can raise interest, there are no guarantees that they do improve the understanding of the fundamental concepts [7].

Resuts and discussions

The results of natural frequencies obtained during simulation analysis and experimental measurement are presented in the table 2.

As it can be seen from table 2, figure 8, the results obtained during simulation analysis and experimental measurement are similar. Both in transversal and radial direction, the difference in natural frequencies of the three studies types of internal spur gears is very small.

In transversal direction the smallest natural frequencies if for the solid body with holes internal spur gear and the highest is for the solid body internal spur gear from both simulation analysis and experimental measurement, but the difference between the two of them is smaller than 1 Hz.

In radial direction the smallest natural frequencies if for goffer type structure internal spur gear and the highest is for the solid body with holes internal spur gear from both

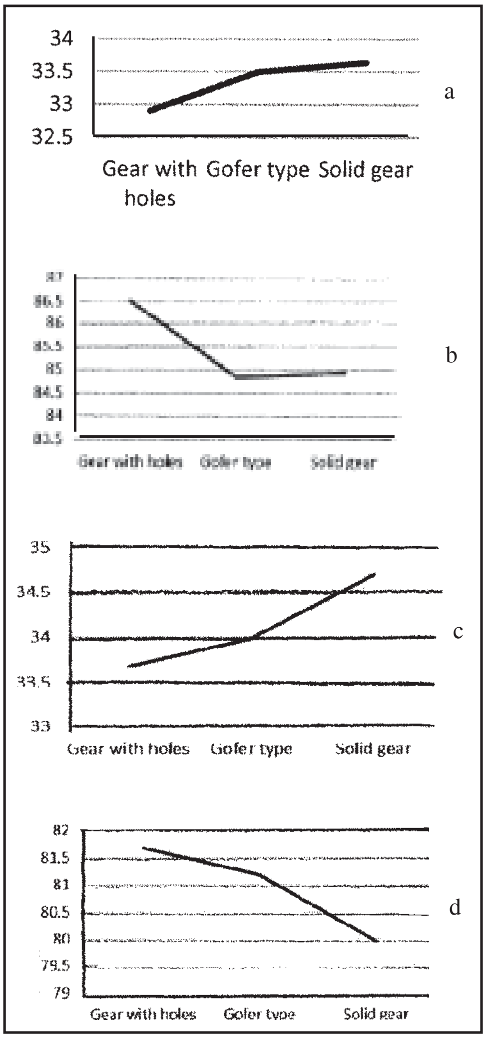

Fig. 8. Results from simulation analysis (a - transversal direction, b - radial direction) and results from experimental measurement (c - transversal direction, d - radial direction)

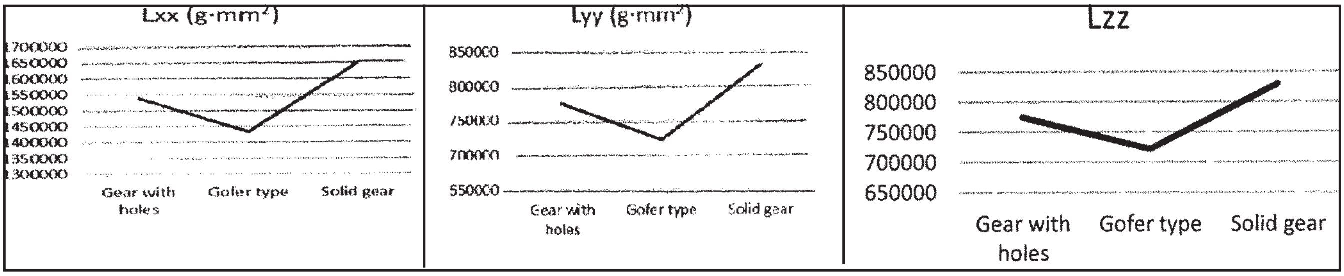

Fig. 9. Moments of inertia taken at the center of mass from CAD model

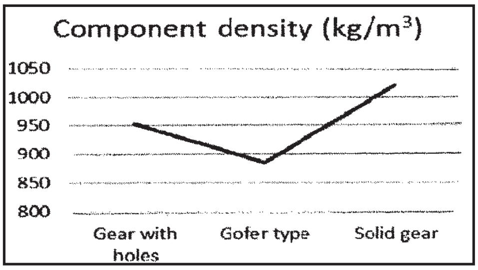

Fig. 10. Component density

simulation analysis and experimental measurement, but the difference between the two of them is smaller than 2 Hz.

By analysing the mass difference between the three solutions for the internal spur gear it can be seen that the goffer type structure internal spur gear is about 13% lighter than the solid body internal spur gear.

Conclusions

From the results presented in this paper we can conclude that we can reduce the mass of the internal spur gear with about 13% without affecting its mechanical resistance and vibrational characteristics.

Acknowledgements. The work has been funded by the Sectorial Operational Programme Human Resources Development 2007-2013 of the Ministry of European Funds through the Financial Agreement POSDRU/159/1.5/S/132397.

References

1. W. LI, Y. LI, Vibration and sound radiation of an asymmetric laminated plate in thermal environments, Acta Mechanica Solida Sinica, 28, No. 1, February, 2015.
2. A.D. LIN, J. H. KUANG, On the Bending and Surface Fatigues of an Engaging Spur Gear Pair, 12th IFToMM World Congress, Besançon (France), June 18-21, 2007.
3. T. KIEKBUSCH, D. SAPPOK, Calculation of the Combined Torsional Mesh Stiffness of Spur Gears with Two- and Three-Dimensional Parametrical FE Models, Journal of Mechanical Engineering 57, 810-818, DOI: 10.5545/sv-jme.2010.248.
4.J. WANG, I. HOWARD, Comprehensive analysis of spur gears in mesh with various types of profile modifications. Proceedings International Conference on Mechanical Transmissions, 42-47.
5. J. WANG, Numerical and experimental analysis of spur gears in mesh. Curtin University, Perth (2003).
6. *** www.matweb.com
7. L. DINESCU, M. DINICA, C. MIRON, E.S. BARNA, The Approach of Teaching and Learning Scanning Electron Microscope in High School Using Virtual Experiments, Rom. Rep. Phys., 65, 2, 588 (2013)

Manuscript received: 16.07.2015